Differentiation of healthy and malignant brain tissues using terahertz pulsed spectroscopy and optical coherence tomography

N.V. Chernomyrdin[a,b], I.N. Dolganova[b,c], S.-I.T. Beshplav[d], P.V. Aleksandrova[b], G.R. Musina[a,b], K.M. Malakhov[a,b], P.V. Nikitin[d], A.V. Kosyr'kova[d], G.A. Komandin[a], I.V. Reshetov[e], A.A. Potapov[d], V.V. Tuchin[f,g,h], and K.I. Zaytsev[a,b]

[a]Prokhorov General Physics Institute of the Russian Academy of Sciences, Moscow 119991, Russia
[b]Bauman Moscow State Technical University, Moscow 105005, Russia
[c]Institute of Solid State Physics of RAS, Chernogolovka 142432, Russia
[d]Burdenko Neurosurgery Institute, Moscow 125047, Russia
[e]Sechenov First Moscow State Medical University, Moscow 119991, Russia
[f]Saratov State University, Department of Optics and Biophotonics, 83 Astrakhanskaya street, Saratov 410012, Russia
[g]Tomsk State University, Interdisciplinary Laboratory of Biophotonics, 36 Lenin avenue, Tomsk 634050, Russia
[h]Institute of Precision Mechanics and Control of RAS, Laboratory of Laser Diagnostics of Technical and Living Systems, 24 Rabochaya street, Saratov 410028, Russia

ABSTRACT

Intraoperative diagnosis of brain tumors remains a challenging problem of modern neurosurgery. A complete resection of tumor is the most important factor, determining an efficiency of its treatment, while an incomplete resection, caused by inaccurate detection of tumor margins, increases a probability of the tumor recurrence. The existing methods of the intraoperative neurodiagnosis of tumors are plagued with limited sensitivity and specificity; they remain laborious, time-consuming and/or rather expensive. Therefore, the development of novel methods for the intraoperative diagnosis of gliomas relying on modern instruments of medical imaging is a topical problem of medicine, physics, and engineering. In our research, we studied the ability of dual-modality imaging that combines such methods as optical coherence tomography (OCT) and terahertz (THz) pulsed spectroscopy, for intraoperative diagnosis of brain tumors with a strong emphasize on a human brain gliomas. We performed experimental studies of the frequency-dependent THz dielectric properties and OCT imaging of healthy (intact) and pathological brain tissues *ex vivo* in order to analyze the prospect for differentiation between tissue classes. The observed results highlight a potential of the considered instruments in the label-free intraoperative neurodiagnostics.

Keywords: terahertz radiation, terahertz pulsed spectroscopy, optical coherence tomography, human brain tumor, malignant glioma, intraoperative diagnosis, gelatin embedding

1. INTRODUCTION

One of the principal problems of the present-day neurosurgery is intraoperative diagnosis of brain gliomas.[1] Efficiency of the therapy strongly depends on the gross total resection of the tumor, and thus it is important to accurately reveal glioma margins.[2] Several methods have already been applied to differentiate healthy

Further author information:
N.V.C.: E-mail: chernik-a@yandex.ru; K.I.Z.: E-mail: kirzay@gmail.com

Clinical and Translational Neurophotonics 2019, edited by Steen J. Madsen, Victor X. D. Yang, Nitish V. Thakor, Proc. of SPIE Vol. 10864, 1086406 · © 2019 SPIE · CCC code: 1605-7422/19/$18 · doi: 10.1117/12.2506600

brain tissues and gliomas, among them magnetic resonance imaging (MRI),[3] Raman spectroscopy,[4] and fluorescent imaging based on fluorescence of protoporphyrin IX (PpIX) accumulated in gliomas under the action of 5-aminolevulinic acid (5-ALA).[5,6] Nevertheless, existing tools are rather expensive, massive, time consuming and/or do not provide satisfactory sensitivity and specificity. Combining diagnostic information from several cutting-edge modalities of medical imaging could become a good solution of this problem. Terahertz (THz) pulsed spectroscopy (TPS)[7] and optical coherence tomography (OCT)[8–10] are prospective tools to differentiate healthy brain tissues and malignant glioma. One of the major advantages of these techniques is an ability to reveal endogenous contrast between healthy and pathological tissues, which means that such methods do not require any labels. These two methods are based on different principles of electromagnetic wave interaction with matter (in particular with biological tissues); thus potentially lead to obtaining more features of malignancies.

THz radiation interacts with vibrational and rotational modes of molecules, which allows one to observe "ingerprints" in THz spectra of numerous biomolecules.[7,11–13] The contrast in THz properties of healthy and pathological tissues is considered to be primarily determined by higher water content in tumors,[14–16] which results in higher refractive index and absorption coefficient of tumors comparing to healthy tissues. But reportedly it also can be affected by lower lipid content[17,18] and higher cell nuclei density per volume unit in cancerous tissues.[19] It was shown that methods of THz imaging and spectroscopy are viable tools for diagnosis of different types of tissue tumors: skin,[20–22] breast,[23,24] colon tissue,[25,26] etc. One of the most dynamical branches of THz biomedical applications today is diagnosis of brain gliomas possessing different grades according to WHO (World Health Organization) classification.[27–31] Previously an ability to differentiate healthy brain tissues and gliomas was demonstrated for paraffin-embedded mouse model tissues,[28] for rat model of brain glioma *in vivo* and *in vitro* and for human brain tissues *in vitro*.[31] Now the most important challenges of THz neurodiagnosis are collecting the database of THz characteristics of human brain gliomas possessing different grades and development of instruments for intraoperative diagnosis including design of effective THz waveguides.[32–34]

OCT systems usually operate in visible or near-infrared (IR) ranges and are based on interferometric detection of backscattered light in medium. This method is sensitive to micrometer-scale tissue inhomogeneities, due to high spatial resolution, and can be used for measuring tissue scattering properties. It is known that scattering coefficient varies for healthy and pathological tissues which results from different cell density.[35,36] Some modalities of OCT were applied for diagnosis of skin,[37,38] prostate,[39] liver[40] tissue diseases, etc. Nowadays methods of OCT are widely applied in clinics for diagnosis of eye corneal and retinal diseases.[41,42] Recently, OCT was applied for studying *in vivo* and *ex vivo* brain diseases[43–46] and particularly for diagnosis of brain glioma.[47–50]

Abovementioned shows that combining TPS and OCT would provide a significant amount of information on endogenous contrast of brain gliomas and healthy brain tissues and would allow to emphasize prominent principal components during further processing. In our study we suggest combining the benefits of TPS and OCT for diagnosis of human brain gliomas. In this pilot research, we study several samples of freshly excised human brain gliomas and healthy (intact) brain tissues using TPS setup operating in reflection mode and OCT system operating in near-IR range during first four hours after surgery. We applied embedding of freshly excised brain tissues in gelatin slabs in order to prevent tissue hydration/dehydration and thus to conserve THz properties of tissues unaltered for several hours after resection. We reconstructed THz refractive indexes and absorption coefficients of healthy (intact) brain tissues and gliomas. After that we obtained OCT images of brain gliomas possessing different grades (I to IV) and intact brain tissue samples and statistically analyzed scattering profiles of OCT scans. Thus, in the present paper, we considered an ability for development intraoperative label-free tool for brain glioma diagnosis based on TPS and OCT.

2. TERAHERTZ DIELECTRIC SPECTROSCOPY OF BRAIN GLIOMAS

2.1 Sample preparation

In the present research, we considered more than 20 samples of human brain tissues, namely: 19 glioma samples possessing different WHO grades (3 samples for grade I, 5 grade II, 3 grade III and 8 grade IV glioma) and 4 healthy (perifocal) brain tissue samples. Brain tissue samples were provided by Burdenko Neurosurgery Institute. Resections were implemented using fluorescence of PpIX induced by 5-ALA. In our study, we applied TPS to differentiate high-grade gliomas and intact tissues, and OCT to distinguish intact tissue, low-grade and high-grade gliomas. Low-grade (I-II) and high-grade (III-IV) brain gliomas demonstrate low contrast of THz dielectric properties. In order to prevent tissue hydration/dehydration[16] all samples were embedded using gelatin slabs[51] right after the resection. After that brain tissues were fixed in formalin and transported to hystological examination, where preliminary diagnoses were approved using hematoxylin and eosin (H&E) stained microscopy.

2.2 Measurement of THz dielectric properties

THz dielectric properties of brain tissue samples were measured using TPS setup based on LT-GaAs photoconductive antennas applied both for generating and for detecting of broadband THz pulses. THz pulses were focused by off-axis parabolic mirror on the sample placed on the reference quartz window. The sample was covered by the gelatin slab in order to isolate brain tissue from atmosphere. The TPS setup was covered by a cube and the atmosphere inside was purged by nitrogen preventing THz wave absorption by water vapors of the air.

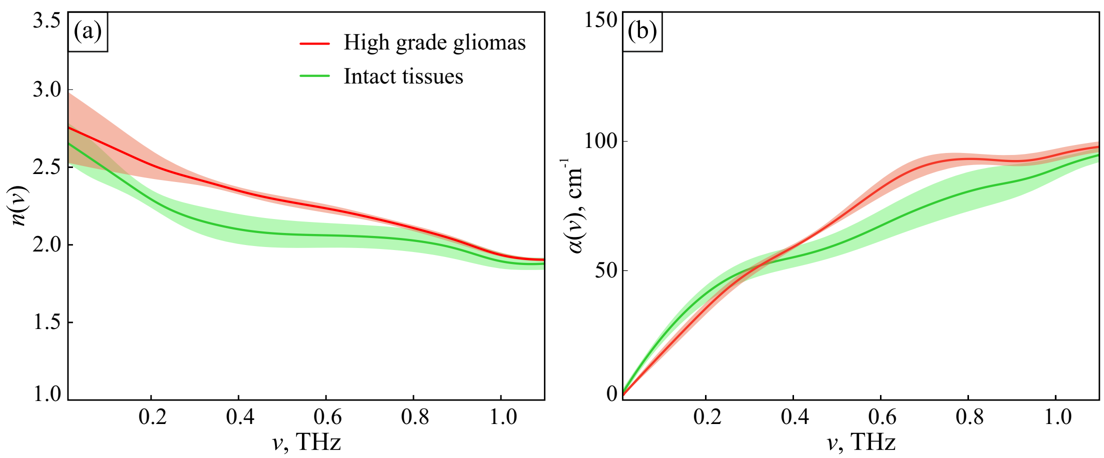

Figure 1. Results for THz pulsed spectroscopy of human brain tissues embedded in gelatin: (a) refractive indexes and (b) absorption coefficients of healthy (intact) brain tissues and high grade gliomas.

We used a method for THz absorption coefficient and refractive index reconstruction described in Refs.[22,52] To solve this inverse ill-posed problem, three signals need to be detected: reflected from reference window E_{R}, from reference window and golden mirror behind it E_{M}, and from reference window and tissue sample behind it E_{S}. THz complex refractive index $\widetilde{n} = n - i\frac{c}{2\pi\nu}\alpha$ was reconstructed by minimizing the error functional, defined as the difference between the experimentally obtained transfer function $\tilde{H}_{exp}$ and the model one $\tilde{H}_{th}$:

$$\Phi = \Big| |\tilde{H}_{exp} - \tilde{H}_{th}|^2 + |\phi[\tilde{H}_{exp}] - \phi[\tilde{H}_{th}]|^2 \Big|. \quad (1)$$

here |...| and ϕ[...] stand for modulus and phase of the function. Fig. 1 demonstrates the average reconstructed refractive indexes (a) and absorption coefficients (b) of intact brain tissues and high grade brain gliomas. Efficient frequency range from 0.1 to 1.1 THz is limited by the diffraction limit of focusing system. We considered possible spatial inhomogeneity of tissue samples by making measurements in several points of tissue surface. Standard deviation of dielectric properties of each sample is depicted by error bars on the graphs. The obtained curves are in a good agreement with the previously reported ones.[30] We can note the contrast of refractive index and absorption coefficient of intact tissue and brain glioma, caused by higher water content and structural changes in pathological tissue. The most significant differences are observed in the frequency range from 0.3 to 0.7 THz. This could become an advantage for THz intraoperative neurodiagnosis of human brain gliomas using endogenous contrast of healthy and pathological tissues.

3. OPTICAL COHERENCE TOMOGRAPHY OF BRAIN GLIOMAS

For the OCT measurements we apply OCT1300Y system, developed by Institute of Applied Physics RAS, Nizny Novgorod, Russia.[53,54] This setup operates at central wavelength of the source equal to 1300 nm and average power of radiation 0.75 mW. A single scan contains 256×400 pixels, corresponding to lateral scanning region of 2 mm. Theoretically achievable spatial resolution in lateral and depth dimensions (in air) is 50 μm and 30 μm, respectively. The measurement process implied registering of OCT images of intact brain tissues and glioma samples, and statistical processing of obtained OCT scans.

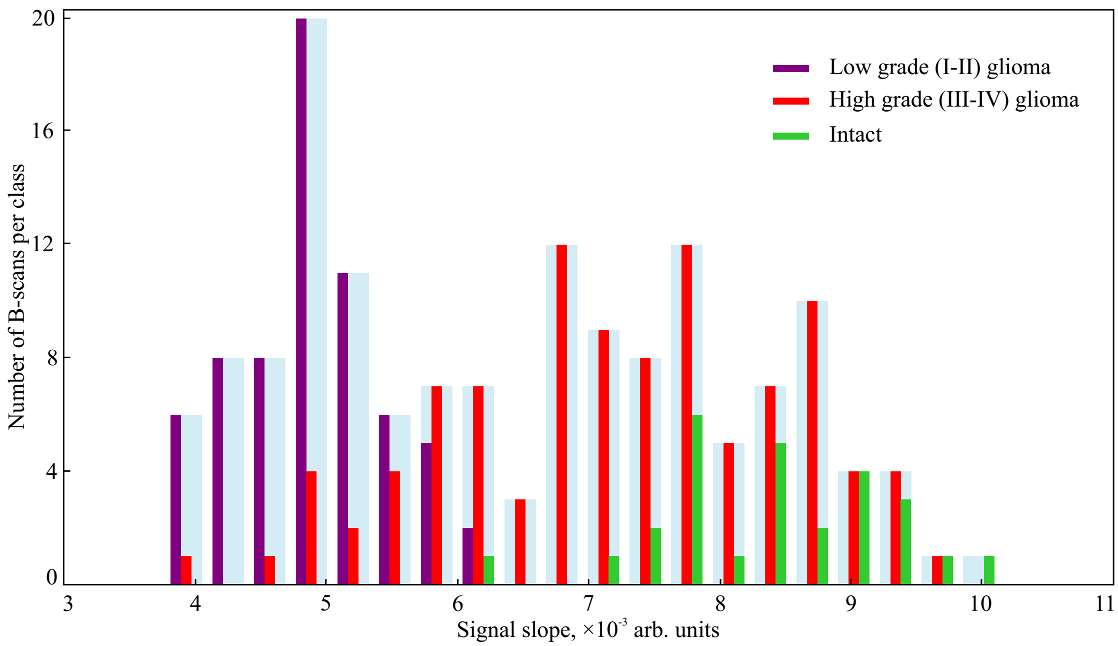

Figure 2. OCT data analysis: histogram depicts distribution of slope-parameter for intact brain tissues, low and high grade gliomas.

It was shown that glioma and intact brain tissue possess different scattering properties, which can be sensed by OCT. In present study, we obtained 22 B-scans of intact brain tissues, 66 scans of low grade (I-II) glioma samples and 125 scans of high grade (III-IV) glioma samples. The measurement of scattering characteristics was based on the analysis of OCT-signal slopes within each A-scan in log-scale and its averaging for each B-scan. The obtained statistics for the considered tissue classes is demonstrated in Fig. 2. A good separability was obtained between low-grade glioma and intact tissue classes as well as between low-grade and high-grade gliomas, while high-grade gliomas and intact tissues could be hardly separated. This means that methods of TPS can be applied to distinguish intact tissues and high grade gliomas, and OCT can be used for differentiating low- and high-grades.

4. DISCUSSIONS

The observed results show a potential of combining OCT and TPS methods for intraoperative diagnosis of malignant brain gliomas relying on detecting of endogenous contrast. The combination of modalities based on different mechanisms of light-matter interactions should improve accuracy of neurodiagnosis. Data complexing and correlation analysis of TPS and OCT characteristics should be studied in a further research.

One of the essential drawbacks of TPS and OCT in medical diagnosis is a limited penetration depth of electromagnetic waves into biological tissues, caused by strong absorption of THz waves by water molecules and by scattering of visible and near-IR light on cell structures of tissues. Immersion optical clearing agents can be used for penetration depth enhancement by matching refractive indexes of tissue scatterers and surrounding media (interstitial field), which is essential in near-IR region[55–58] and by reduction of water content in tissues, essential for THz frequency range.[59–62]

5. CONCLUSIONS

We applied the methods of TPS and OCT *ex vivo* to study their possibility of differentiating intact human brain tissues and gliomas possessing low and high grades of malignancy. We detected THz signals of brain tissues using pulsed spectrometer operating in reflection mode, and reconstructed THz refractive indexes and absorption coefficients using the algorithm for solving the inverse ill-posed problem. After that, we obtained OCT images of the brain tissue samples and applied statistical approach to emphasize contrast in scattering properties of intact brain tissues and different grades of brain gliomas. Both TPS and OCT demonstrated an ability to differentiate intact brain tissues and gliomas, relying only on endogenous contrast of optical characteristics. Thereby, this work yields preliminary analysis (feasibility test), which aims to objectively uncover strengths and weaknesses of TPS and OCT from the purpose of their use in intraoperative diagnosis of human brain tumors before committing to a full-blown study involving measurements and analysis of a large amount of tissue samples, both *ex vivo* and *in vivo*.

ACKNOWLEDGMENTS

THz pulsed spectroscopy of human brain gliomas was supported by Russian Foundation for Basic Research (RFBR), Project # 18-38-00504; study of brain tissues using optical coherence tomography was sponsored by RFBR Project # 18-38-00853.

REFERENCES

[1] Ostrom, Q. T., Gittleman, H., Liao, P., Vecchione-Koval, T., Wolinsky, Y., Kruchko, C., and Barnholtz-Sloan, J. S., "CBTRUS Statistical Report: Primary brain and other central nervous system tumors diagnosed in the United States in 20102014," *Neuro-Oncology* **19**(suppl_5), v1–v88 (2017).

[2] Phuphanich, S., Ferrall, S., and Greenberg, H., "Long-term survival in malignant glioma. Prognostic factors," *Journal of the Florida Medical Association* **80**(3), 181–184 (1993).

[3] Senft, C., Bink, A., Franz, K., Vatter, H., Gasser, T., and Seifert, V., "Intraoperative MRI guidance and extent of resection in glioma surgery: A randomised, controlled trial," *The Lancet Oncology* **12**(11), 997–1003 (2011).

[4] Kircher, M. F., De La Zerda, A., Jokerst, J. V., Zavaleta, C. L., Kempen, P. J., Mittra, E., Pitter, K., Huang, R., Campos, C., Habte, F., Sinclair, R., Brennan, C. W., Mellinghoff, I. K., Holland, E. C., and Gambhir, S. S., "A brain tumor molecular imaging strategy using a new triple-modality MRI-photoacoustic-Raman nanoparticle," *Nature Medicine* **18**(5), 829–834 (2012).

[5] Stummer, W., Pichlmeier, U., Meinel, T., Wiestler, O. D., Zanella, F., and Reulen, H.-J., "Fluorescence-guided surgery with 5-aminolevulinic acid for resection of malignant glioma: a randomised controlled multicentre phase III trial," *The Lancet Oncology* **7**(5), 392–401 (2006).

[6] Schatlo, B., Fandino, J., Smoll, N., Wetzel, O., Remonda, L., Marbacher, S., Perrig, W., Landolt, H., and Fathi, A.-R., "Outcomes after combined use of intraoperative MRI and 5-aminolevulinic acid in high-grade glioma surgery," *Neuro-Oncology* **17**(12), 1560–1567 (2015).

[7] Smolyanskaya, O. A., Chernomyrdin, N. V., Konovko, A. A., Zaytsev, K. I., Ozheredov, I. A., Cherkasova, O. P., Nazarov, M. M., Guillet, J.-P., Kozlov, S. A., Kistenev, Y. V., Coutaz, J.-L., Mounaix, P., Vaks, V. L., Son, J.-H., Cheon, H., Wallace, V. P., Feldman, Y., Popov, I., Yaroslavsky, A. N., Shkurinov, A. P., and Tuchin, V. V., "Terahertz biophotonics as a tool for studies of dielectric and spectral properties of biological tissues and liquids," *Progress in Quantum Electronics* **62**, 1–77 (2018).

[8] Huang, D., Swanson, E. A., Lin, C. P., Schuman, J. S., Stinson, W. G., Chang, W., Hee, M. R., Flotire, T., Gregory, T., Pulifito, C. A., Fujimoto, J. G., Flotte, T., Gregory, K., Puliafito, C. A., and Fujimoto, J. G., "Optical Coherence Tomography," *Science* **254**(5035), 1178–1181 (1991).

[9] Carrasco-Zevallos, O. M., Viehland, C., Keller, B., Draelos, M., Kuo, A. N., Toth, C. A., and Izatt, J. A., "Review of intraoperative optical coherence tomography: technology and applications [Invited]," *Biomedical Optics Express* **8**(3), 1607 (2017).

[10] Tomlins, P. H. and Wang, R. K., "Theory, developments and applications of optical coherence tomography," *Journal of Physics D: Applied Physics* **38**(15), 2519–2535 (2005).

[11] Özer, Z., Gök, S., Altan, H., and Severcan, F., "Concentration-Based Measurement Studies of L-Tryptophan Using Terahertz Time-Domain Spectroscopy (THz-TDS)," *Applied Spectroscopy* **68**(1), 95–100 (2014).

[12] Markelz, A. G., Roitberg, A., and Heilweil, E. J., "Pulsed terahertz spectroscopy of DNA, bovine serum albumin and collagen between 0.1 and 2.0 THz," *Chemical Physics Letters* **320**(1–2), 42–48 (2000).

[13] Funkner, S., Niehues, G., Schmidt, D. A., Heyden, M., Schwaab, G., Callahan, K. M., Tobias, D. J., and Havenith, M., "Watching the low-frequency motions in aqueous salt solutions: the terahertz vibrational signatures of hydrated ions," *Journal of the American Chemical Society* **134**(2), 1030–1035 (2012).

[14] Chen, H., Chen, T.-H., Tseng, T.-F., Lu, J.-T., Kuo, C.-C., Fu, S.-C., Lee, W.-J., Tsai, Y.-F., Huang, Y.-Y., Chuang, E. Y., Hwang, Y.-J., Sun, C.-K., Huan, Y.-Y., Chuang, E. Y., Hwang, Y.-J., and Sun, C.-K., "High-sensitivity in vivo THz transmission imaging of early human breast cancer in a subcutaneous xenograft mouse model," *Optics Express* **19**(22), 21552–21562 (2011).

[15] Pickwell, E., Cole, B. E., Fitzgerald, A. J., Wallace, V. P., and Pepper, M., "Simulation of terahertz pulse propagation in biological systems," *Applied Physics Letters* **84**(12), 2190–2192 (2004).

[16] Png, G. M., Choi, J. W., Ng, B. W.-H., Mickan, S. P., Abbott, D., and Zhang, X.-C., "The impact of hydration changes in fresh bio-tissue on THz spectroscopic measurements," *Physics in Medicine and Biology* **53**(13), 3501–3517 (2008).

[17] Yates, A. J., Thompson, D. K., Boesel, C. P., Albrightson, C., and Hart, R. W., "Lipid composition of human neural tumors," *Journal of Lipid Research* **20**(4), 428–436 (1979).

[18] Köhler, M., MacHill, S., Salzer, R., and Krafft, C., "Characterization of lipid extracts from brain tissue and tumors using Raman spectroscopy and mass spectrometry," *Analytical and Bioanalytical Chemistry* **393**(5), 1513–1520 (2009).

[19] Yamaguchi, S., Fukushi, Y., Kubota, O., Itsuji, T., Ouchi, T., and Yamamoto, S., "Origin and quantification of differences between normal and tumor tissues observed by terahertz spectroscopy," *Physics in Medicine and Biology* **61**(18), 6808 (2016).

[20] Woodward, R. M., Cole, B. E., Wallace, V. P., Pye, R. J., Arnone, D. D., Linfield, E. H., and Pepper, M., "Terahertz pulse imaging in reflection geometry of human skin cancer and skin tissue," *Physics in Medicine and Biology* **47**(21), 3853–3863 (2002).

[21] Woodward, R. M., Wallace, V. P., Pye, R. J., Cole, B. E., Arnone, D. D., Linfield, E. H., and Pepper, M., "Terahertz pulse imaging of ex vivo basal cell carcinoma," *Journal of Investigative Dermatology* **120**(1), 72–78 (2003).

[22] Zaytsev, K. I., Kudrin, K. G., Karasik, V. E., Reshetov, I. V., and Yurchenko, S. O., "In vivo terahertz spectroscopy of pigmentary skin nevi: Pilot study of non-invasive early diagnosis of dysplasia," *Applied Physics Letters* **106**(5), 053702 (2015).

[23] Fitzgerald, A. J., Wallace, V. P., Jimenez-Linan, M., Bobrow, L., Pye, R. J., Purushotham, A. D., and Arnone, D. D., "Terahertz pulsed imaging of human breast tumors," *Radiology* **239**(2), 533–540 (2006).

[24] Ashworth, P. C., Pickwell-MacPherson, E., Provenzano, E., Pinder, S. E., Purushotham, A. D., Pepper, M., and Wallace, V. P., "Terahertz pulsed spectroscopy of freshly excised human breast cancer," *Optics Express* **17**(15), 12444 (2009).

[25] Doradla, P., Alavi, K., Joseph, C. S., and Giles, R. H., "Detection of colon cancer by continuous-wave terahertz polarization imaging technique," *Journal of Biomedical Optics* **18**(9), 90504 (2013).

[26] Wahaia, F., Kasalynas, I., Seliuta, D., Molis, G., Urbanowicz, A., Carvalho Silva, C. D., Carneiro, F., Valusis, G., and Granja, P. L., "Study of paraffin-embedded colon cancer tissue using terahertz spectroscopy," *Journal of Molecular Structure* **1079**, 448–453 (2015).

[27] Png, G. M., Flook, R., Ng, B. W.-H., and Abbott, D., "Terahertz spectroscopy of snap-frozen human brain tissue: an initial study," *Electronics Letters* **45**(7), 343 (2009).

[28] Meng, K., Chen, T.-N., Chen, T., Zhu, L.-G., Liu, Q., Li, Z., Li, F., Zhong, S.-c., Li, Z.-R., Feng, H., and Zhao, J.-H., "Terahertz pulsed spectroscopy of paraffin-embedded brain glioma," *Journal of Biomedical Optics* **19**(7), 077001 (2014).

[29] Oh, S. J., Kim, S.-H., Ji, Y. B., Jeong, K., Park, Y., Yang, J., Park, D. W., Noh, S. K., Kang, S.-G., Huh, Y.-M., Son, J.-H., and Suh, J.-S., "Study of freshly excised brain tissues using terahertz imaging," *Biomedical Optics Express* **5**(8), 2837 (2014).

[30] Yamaguchi, S., Fukushi, Y., Kubota, O., Itsuji, T., Ouchi, T., and Yamamoto, S., "Brain tumor imaging of rat fresh tissue using terahertz spectroscopy," *Scientific Reports* **6**(1), 30124 (2016).

[31] Ji, Y. B., Oh, S. J., Kang, S.-G., Heo, J., Kim, S.-H., Choi, Y., Song, S., Son, H. Y., Kim, S. H., Lee, J. H., Haam, S. J., Huh, Y. M., Chang, J. H., Joo, C., and Suh, J.-S., "Terahertz reflectometry imaging for low and high grade gliomas," *Scientific Reports* **6**, 36040 (2016).

[32] Zaytsev, K. I., Katyba, G. M., Kurlov, V. N., Shikunova, I. A., Karasik, V. E., and Yurchenko, S. O., "Terahertz photonic crystal waveguides based on sapphire shaped crystals," *IEEE Transactions on Terahertz Science and Technology* **6**(4), 576–582 (2016).

[33] Katyba, G. M., Zaytsev, K. I., Dolganova, I. N., Shikunova, I. A., Chernomyrdin, N. V., Yurchenko, S. O., Komandin, G. A., Reshetov, I. V., Nesvizhevsky, V. V., and Kurlov, V. N., "Sapphire shaped crystals for waveguiding, sensing and exposure applications," *Progress in Crystal Growth and Characterization of Materials* **64**(4), 133–151 (2018).

[34] Katyba, G. M., Zaytsev, K. I., Chernomyrdin, N. V., Shikunova, I. A., Komandin, G. A., Anzin, V. B., Lebedev, S. P., Spektor, I. E., Karasik, V. E., Yurchenko, S. O., Reshetov, I. V., Kurlov, V. N., and Skorobogatiy, M., "Sapphire photonic crystal waveguides for terahertz sensing in aggressive environments," *Advanced Optical Materials* **6**, 1800573 (2018).

[35] Fercher, A. F., Drexler, W., Hitzenberger, C. K., and Lasser, T., "Optical coherence tomography - principles and applications," *Reports on Progress in Physics* **66**(2), 239–303 (2003).

[36] Fujimoto, J. G., "Optical coherence tomography for ultrahigh resolution in vivo imaging," *Nature Biotechnology* **21**(11), 1361–1367 (2003).

[37] Welzel, J., "Optical coherence tomography in dermatology: a review," *Skin Research and Technology* **7**(1), 1–9 (2001).

[38] Shlivko, I. L., Kirillin, M. Y., Donchenko, E. V., Ellinsky, D. O., Garanina, O. E., Neznakhina, M. S., Agrba, P. D., and Kamensky, V. A., "Identification of layers in optical coherence tomography of skin: comparative analysis of experimental and Monte Carlo simulated images," *Skin Research and Technology* **21**(4), 419–425 (2015).

[39] Muller, B. G., de Bruin, D. M., van den Bos, W., Brandt, M. J., Velu, J. F., Bus, M. T. J., Faber, D. J., Savci, D., Zondervan, P. J., de Reijke, T. M., Pes, P. L., de la Rosette, J., and van Leeuwen, T. G., "Prostate cancer diagnosis: the feasibility of needle-based optical coherence tomography," *Journal of Medical Imaging* **2**(3), 037501 (2015).

[40] Zhu, Y., Gao, W., Zhou, Y., Guo, Y., Guo, F., and He, Y., "Rapid and high-resolution imaging of human liver specimens by full-field optical coherence tomography," *Journal of Biomedical Optics* **20**(11), 116010 (2015).

[41] Bagayev, S. N., Gelikonov, V. M., Gelikonov, G. V., Kargapoltsev, E. S., Kuranov, R. V., Razhev, A. M., Turchin, I. V., and Zhupikov, A. A., "Optical coherence tomography for in situ monitoring of laser corneal ablation," *Journal of Biomedical Optics* **7**(4), 633 (2002).

[42] Cua, M., Lee, S., Miao, D., Ju, M. J., Mackenzie, P. J., Jian, Y., and Sarunic, M. V., "Retinal optical coherence tomography at 1 μm with dynamic focus control and axial motion tracking," *Journal of Biomedical Optics* **21**(2), 026007 (2016).

[43] Baran, U. and Wang, R. K., "Review of optical coherence tomography based angiography in neuroscience," *Neurophotonics* **3**(1), 010902 (2016).

[44] Assayag, O., Grieve, K., Devaux, B., Harms, F., Pallud, J., Chretien, F., Boccara, C., and Varlet, P., "Imaging of non-tumorous and tumorous human brain tissues with full-field optical coherence tomography," *NeuroImage: Clinical* **2**, 549–557 (2013).

[45] Kut, C., Chaichana, K. L., Xi, J., Raza, S. M., Ye, X., McVeigh, E. R., Rodriguez, F. J., Quiñones-Hinojosa, A., and Li, X., "Detection of human brain cancer infiltration ex vivo and in vivo using quantitative optical coherence tomography," *Science Translational Medicine* **7**(292), 292ra100–292ra100 (2015).

[46] Lichtenegger, A., Harper, D. J., Augustin, M., Eugui, P., Muck, M., Gesperger, J., Hitzenberger, C. K., Woehrer, A., and Baumann, B., "Spectroscopic imaging with spectral domain visible light optical coherence microscopy in Alzheimer's disease brain samples," *Biomedical Optics Express* **8**(9), 4007 (2017).

[47] Yashin, K. S., Kiseleva, E. B., Gubarkova, E. V., Matveev, L. A., Karabut, M. M., Elagin, V. V., Sirotkina, M. A., Medyanik, I. A., Kravets, L. Y., and Gladkova, N. D., "Multimodal optical coherence tomography for in vivo imaging of brain tissue structure and microvascular network at glioblastoma," *Proceedings of SPIE* **10050**, 100500Z (2017).

[48] Yashin, K. S., Karabut, M. M., Fedoseeva, V. V., Khalansky, A. S., Matveev, L. A., Elagin, V. V., Kuznetsov, S. S., Kiseleva, E. B., Kravets, L. Y., Medyanik, I. ., and Gladkova, N. D., "Multimodal optical coherence tomography in visualization of brain tissue structure at glioblastoma (experimental study)," *Sovremennye Tehnologii v Medicine* **8**(1), 73–81 (2016).

[49] Yuan, W., Kut, C., Liang, W., and Li, X., "Robust and fast characterization of OCT-based optical attenuation using a novel frequency-domain algorithm for brain cancer detection," *Scientific Reports* **7**(1), 44909 (2017).

[50] Böhringer, H. J., Boller, D., Leppert, J., Knopp, U., Lankenau, E., Reusche, E., Hüttmann, G., and Giese, A., "Time-domain and spectral-domain optical coherence tomography in the analysis of brain tumor tissue," *Lasers in Surgery and Medicine* **38**(6), 588–597 (2006).

[51] Fan, S., Ung, B., Parrott, E. P. J., and Pickwell-MacPherson, E., "Gelatin embedding: a novel way to preserve biological samples for terahertz imaging and spectroscopy," *Physics in Medicine and Biology* **60**(7), 2703–2713 (2015).

[52] Zaytsev, K. I., Gavdush, A. A., Chernomyrdin, N. V., and Yurchenko, S. O., "Highly accurate in vivo terahertz spectroscopy of healthy skin: variation of refractive index and absorption coefficient along the human body," *IEEE Transactions on Terahertz Science and Technology* **5**(5), 817–827 (2015).

[53] Gelikonov, V. M., Gelikonov, G. V., Gladkova, N. D., Kuranov, R. V., Nikulin, N. K., Petrova, G. A., Pochinko, V. V., Pravdenko, K. I., Sergeev, A. M., Fel'dshtem, F. I., Khanin, Y. I., and Shabanov, D. V., "Coherent optical tomography of microscopic inhomogeneities in biological tissues," *JETP Letters* **61**(2), 158–162 (1995).

[54] Turchin, I. V., Sergeeva, E. A., Dolin, L. S., Kamensky, V. A., Shakhova, N. M., and Richards-Kortum, R., "Novel algorithm of processing optical coherence tomography images for differentiation of biological tissue pathologies," *Journal of Biomedical Optics* **10**(6), 064024 (2005).

[55] Tuchin, V. V., [*Tissue Optics: Light Scattering Methods and Instruments for Medical Diagnostics*], SPIE Press, Bellingham, Washington, USA (2007).

[56] Tuchin, V. V., [*Handbook of Optical Biomedical Diagnostics.Volume 1: Light - Tissue Interaction*], SPIE Press, Bellingham, Washington, USA (2016).

[57] Wang, H., Magnain, C., Wang, R., Dubb, J., Varjabedian, A., Tirrell, L. S., Stevens, A., Augustinack, J. C., Konukoglu, E., Aganj, I., Frosch, M. P., Schmahmann, J. D., Fischl, B., and Boas, D. A., "as-PSOCT: Volumetric microscopic imaging of human brain architecture and connectivity," *NeuroImage* **165**, 56–68 (2018).

[58] Larin, K. V., Ghosn, M. G., Bashkatov, A. N., Genina, E. A., Trunina, N. A., and Tuchin, V. V., "Optical clearing for OCT image enhancement and in-depth monitoring of molecular diffusion," *IEEE Journal of Selected Topics in Quantum Electronics* **18**(3), 1244–1259 (2012).

[59] Oh, S. J., Kim, S.-H., Jeong, K., Park, Y., Huh, Y.-M., Son, J.-H., and Suh, J.-S., "Measurement depth enhancement in terahertz imaging of biological tissues," *Optics Express* **21**(18), 21299 (2013).

[60] Kolesnikov, A. S., Kolesnikova, E. A., Kolesnikova, K. N., Tuchina, D. K., Popov, A. P., Skaptsov, A. A., Nazarov, M. M., Shkurinov, A. P., Terentyuk, A. G., and Tuchin, V. V., "THz monitoring of the dehydration of biological tissues affected by hyperosmotic agents," *Physics of Wave Phenomena* **22**(3), 169–176 (2014).

[61] Smolyanskaya, O. A., Schelkanova, I. J., Kulya, M. S., Odlyanitskiy, E. L., Goryachev, I. S., Tcypkin, A. N., Grachev, Y. V., Toropova, Y. G., and Tuchin, V. V., "Glycerol dehydration of native and diabetic animal tissues studied by THz-TDS and NMR methods," *Biomedical Optics Express* **9**(3), 1198 (2018).

[62] Malakhov, K. M., Tuchin, V. V., Tuchina, D. K., Chuchupal, S. V., Cherkasova, O. P., Dolganova, I. N., Chernomyrdin, N. V., Zaytsev, K. I., Gavdush, A. A., Musina, G. R., and Komandin, G. A., "Terahertz spectroscopy of immersion optical clearing agents: DMSO, PG, EG, PEG," *Proceedings of SPIE* **10800**, 108000F (2018).